A Computational Approach to the Study of the Binding Mode of Dual ACE/NEP Inhibitors

Nikolaos Dimitropoulos,[†] Athanasios Papakyriakou,[†] Georgios A. Dalkas,[†] Edward D. Sturrock,[‡] and Georgios A. Spyroulias*,[†]

Department of Pharmacy, University of Patras, Panepistimioupoli, Rion, GR-26504, Greece, and Division of Medical Biochemistry, Institute of Infectious Disease and Molecular Medicine, University of Cape Town, South Africa

Received December 24, 2009

Combined blockade of the renin−angiotensin−aldosterone system (RAAS) is an attractive therapeutic strategy for the treatment of cardiovascular diseases. Vasopeptidase inhibitors are a group of compounds capable of inhibiting more than one enzyme, which leads to potentiation of natriuretic peptide actions and suppression of the RAAS. In this study, molecular modeling has been used to elucidate key structural features that govern the binding and/or selectivity of a single compound toward the zinc catalytic sites of the N- and C-domains of the angiotensin-converting enzyme (ACE) and the neutral endopeptidase (NEP). Eleven dual inhibitors were categorized in three classes, according to their zinc binding groups. Analysis of their docked conformers revealed the molecular environment of the catalytic sites and the specific interactions between the inhibitors and amino acid residues that are important for selectivity and cooperativity. In addition, inhibitors were predicted to bind to the C-domain of the ACE with greater affinity than the N-domain, with an average difference in the free energy of binding ∼2−3 kcal mol^{-1}. Residues that were identified to actively participate in the binding and stabilizating of the enzyme−inhibitor complexes were analyzed in a consensus way for both the ACE and the NEP. These atomic-level insights into enzyme−ligand binding can be used to drive new structure-based drug design processes in the quest for more selective and effective vasopeptidase inhibitors.

INTRODUCTION

Cardiovascular disease (CD) is the primary cause of death in the United States and Europe.[1,2] Hypertension is an important risk factor for CD, while also being associated with other diseases, like chronic kidney disease.[1,2] Blood pressure is regulated mainly by the renin−angiotensin−aldosterone system (RAAS), the natriuretic peptides and kinin system (NPKS), and the endothelin system (ETS).[3,4] In the RAAS, renin, released by the kidney, converts the circulating angiotensinogen to the decapeptide angiotensin I (AI), which in turn is converted to the potent vasoconstrictor angiotensin II (AII) by the angiotensin-converting enzyme (ACE). The NPKS comprises the vasodilators bradykinin (BK, a nonapeptide) and the natriuretic peptides (NPs). In the ETS, the endothelin-converting enzyme (ECE) generates the vasoconstrictor endothelin-1 (ET-1). Neutral endopeptidase (NEP) is implicated in the degradation of AI, AII, BK, ET-1, and NPs.

ACE (EC 3.4.15.1)[5,6] is a zinc metallopeptidase that belongs to the M2 gluzincin family. There are two isoforms of ACE: the somatic form (sACE), found in somatic tissues, and the testicular form (tACE), found in germinal cells.[7] The somatic form is a 1277 amino acid glycoprotein composed of two functionally active domains, C- and N-domain (cACE and nACE, respectively). The tACE is a 701 amino acid isoform that corresponds to the C-domain of the sACE.[8] Each domain contains an active site bearing the consensus HExxH and ExxxD zinc-binding motifs of gluzincins.[9] The two domains of the sACE have a high-degree sequence identity and exhibit similar catalytic activities toward AI and BK. However, the enzymatic activity of the C-domain is highly dependent on the chloride ion concentration, whereas the N-domain is fully activated at relatively low concentrations of the anion.[10,11] The two domains also differ in substrate and inhibitor specificity. For example, the inhibitor RXP407 is 1000 times more specific for the N-domain, while RXPA380 is 3000 times more specific for the C-domain.[12] Because of the central role of ACE in blood pressure regulation, several ACE inhibitors, such as captopril, lisinopril, and enalapril, have been developed.[13,14] These drugs are widely used for the treatment of hypertension and chronic heart failure.[2]

NEP (EC 3.4.24.11)[15,16] is a zinc-containing endopeptidase that belongs to the M13 gluzincin family. This enzyme is found in a wide variety of tissues and has broad selectivity.[17] It is responsible for degrading various signaling peptides, such as endogenous enkephalins, substance P, Atrial natriuretic peptide (ANP), endothelin, and bradykinin and, more recently, has been found to be implicated in the degradation of the amyloid-beta peptide.[15,18] It is a type II membrane protein consisting of a short N-terminal cytoplasmic domain, followed by a single transmembrane helix and a large C-terminal extracellular domain that contains the active site.[19] The C-terminal domain includes the active site with the

* Corresponding author. Telephone: +30 2610969950 951. Fax: +30 2610969950, -951. E-mail: G.A.Spyroulias@upatras.gr.
[†] University of Patras.
[‡] University of Cape Town.

10.1021/ci9005047
Published on Web 02/19/2010

typical HExxH and ExxxD gluzincin motif.[15] Some NEP inhibitors that have been synthesized demonstrate potent pharmacological activity as novel analgesics or antihypertensive agents.[20,21] However, clinical studies involving the use of these inhibitors in humans showed no substantial reduction in blood pressure, either in normotensives or in hypertensives, and only limited beneficial effects in patients with mild chronic heart failure.[22,23] These results might be related to the simultaneous degradation of vasodilator (BK, NPs) and vasoconstrictor peptides (AII, ET-1) by NEP.

Because of their important role in the regulation of the cardiovascular and renal systems, simultaneous inhibition of ACE and NEP has been proposed. Several clinical trials have indicated that the combined administration of ACE and NEP inhibitors results in a greater antihypertensive effect compared to either drug alone.[24,25] Since both ACE and NEP, and also ECE, are zinc metallopeptidases with significant structural homology that regulate the levels of vasoactive peptides, the development of single compounds that exhibit inhibitory activities for two or even all three of the above enzymes has been attempted. These mixed inhibitors are called vasopeptidase inhibitors (VPIs). The first VPIs to enter clinical trials were dual ACE/NEP inhibitors.[4,26]

Several clinical trials in hypertensive patients have shown that dual ACE/NEP inhibitors exert a potent and sustained antihypertensive activity.[4,26] The mechanism of action of these compounds is via inhibition of both ACE and NEP, leading to a synergistic vasodilating effect more potent than that of selective inhibitors alone. However, in the OCTAVE trial, the dual ACE/NEP inhibitor omapatrilat resulted in an increased incidence of the adverse reaction angioedema,[27] stalling the development of these inhibitors. ACE inhibition results in decreased blood levels of the vasoconstrictor AII and increased levels of the vasodilator BK. Reduction of AII levels results in vasodilation through reduced AT1 receptor activation and ET-1 release and through endothelial nitric oxide (NO) production, while increased levels of BK contribute to NO release. NEP inhibition increases the BK and NP levels and, thus, complements the vasodilating effect of ACE inhibition. However, NEP inhibition also results in increased concentrations of the potent vasoconstrictor ET-1.[4,26]

The recently published ligand-free and -bound X-ray structures of ACE and NEP have provided valuable insights into structural determinants of enzyme−inhibitor interactions.[16,28,29] It is likely that more selective novel inhibitors could be developed through structure-based drug design. In the present study, docking simulations were used to predict and investigate interactions of the two ACE domains and NEP with several dual inhibitors in an attempt to elucidate the factors that govern enzyme−ligand binding. In order to evaluate the ability of our docking calculations to reproduce the crystal structures of ACE inhibitors, we carried out a comparison between the docked and the crystallographic conformations of three inhibitors (lisinopril, enalaprilat, and captopril). The predicted free energies of binding showed good correlation with the experimentally determined values, which prompted further analysis of 11 dual inhibitors with C- and N-domains of ACE and NEP.

EXPERIMENTAL SECTION

Structure Preparation. The crystallographic coordinates of the enzymes were obtained from the RCSB Protein Data Bank. PDB ID: 1O86 was used for the C-domain of ACE (cACE), 2C6N for the N-domain of ACE (nACE), and 1R1H for NEP. All crystallographic water molecules, bound inhibitors, and other heteroatoms were removed from the PDB files, with the exception of zinc and chloride ions. Hydrogen and missing atoms were added using the LEaP module of AMBER 9.[30] The protonation state of the ionizable residues was predicted by the program H++, using a continuum electrostatic model based on the Poisson−Boltzmann method.[31] Histidine residues were also visually inspected, so as to identify putative hydrogen-bonding networks with neighboring residues. The parm99 AMBER force field was applied to all protein atoms,[32] while the parameters for zinc and chloride ions were taken from the AMBER database, as described previously.[33] Each system was relaxed using 500 steps of energy minimization with the steepest descent method and using positional restraints of a harmonic force constant $K = 50$ kcal mol^{-1} Å^{-2} on all heavy atoms, except those not determined in the X-ray structure. The generalized Born implicit solvation model (GB^{HCT})[34] was employed with a 16 Å cutoff for the nonbonded interactions.

Coordinates for the ligands from the ACE inhibitor crystal structures retrieved from the PDB files: 1UZF for captopril, 1UZE for enalaprilat, and 1O86 for lisinopril. Hydrogen atoms were added by the program Babel3, and then AM1-BCC partial charges[35] were calculated using the Molcharge module of the OpenEye suite of programs.[36] For the dual inhibitors, where there are no X-ray structures (Scheme 1), the coordinates were obtained from SMILES representation using the program Omega 2.1.[37] AVE7688 was prepared with the free sulfhydryl (SH), since the thioester shown in Scheme 1 is a prodrug. Partial atomic charges were calculated, as described above. The carboxylate and the primary amine groups of the inhibitors were set to their standard ionic state. For inhibitors bearing thiol groups, two separate files for each ligand were prepared, one with the sulfhydryl protonated and the other one deprotonated. Subsequently, docking calculations were performed for both protonation states, and the results were analyzed depending on whether the thiol would be the zinc-binding group. In this case, we have considered the binding energy of the deprotonated form. On the other hand, the binding energy of the protonated SH form is reported.

Docking of the Ligands. AutoDock 3.05[38] was used for the docking calculations, and AutoDockTools 1.5.4[39] was used for visual inspection of the docking results. Proteins and ligands were treated with the united-atom approximation by merging all nonpolar hydrogens. Kollman partial charges were assigned to all protein atoms, while for the zinc and chloride ions, formal charges of +2 and −1 were applied, and their van der Waals parameters were taken from the AMBER database. The grid maps were centered next to zinc and comprised 61 × 61 × 61 points of 0.375 Å spacing. The Lamarckian genetic algorithm was employed with the following parameters: (i) population size of individuals = 150; (ii) maximum number of energy evaluations = 2.5 × 10^6 and maximum number of generations = 27 000; (iii) elitism value = 1; (iv) mutation rate = 0.02; and (v) crossover rate = 0.80.[38] For all the calculations, 100 docking rounds were performed with step sizes of 0.2 Å for translations and with orientations and torsions of 5.0°.

Scheme 1. Three ACE Inhibitors and the Dual ACE/NEP Inhibitors Used in This Study

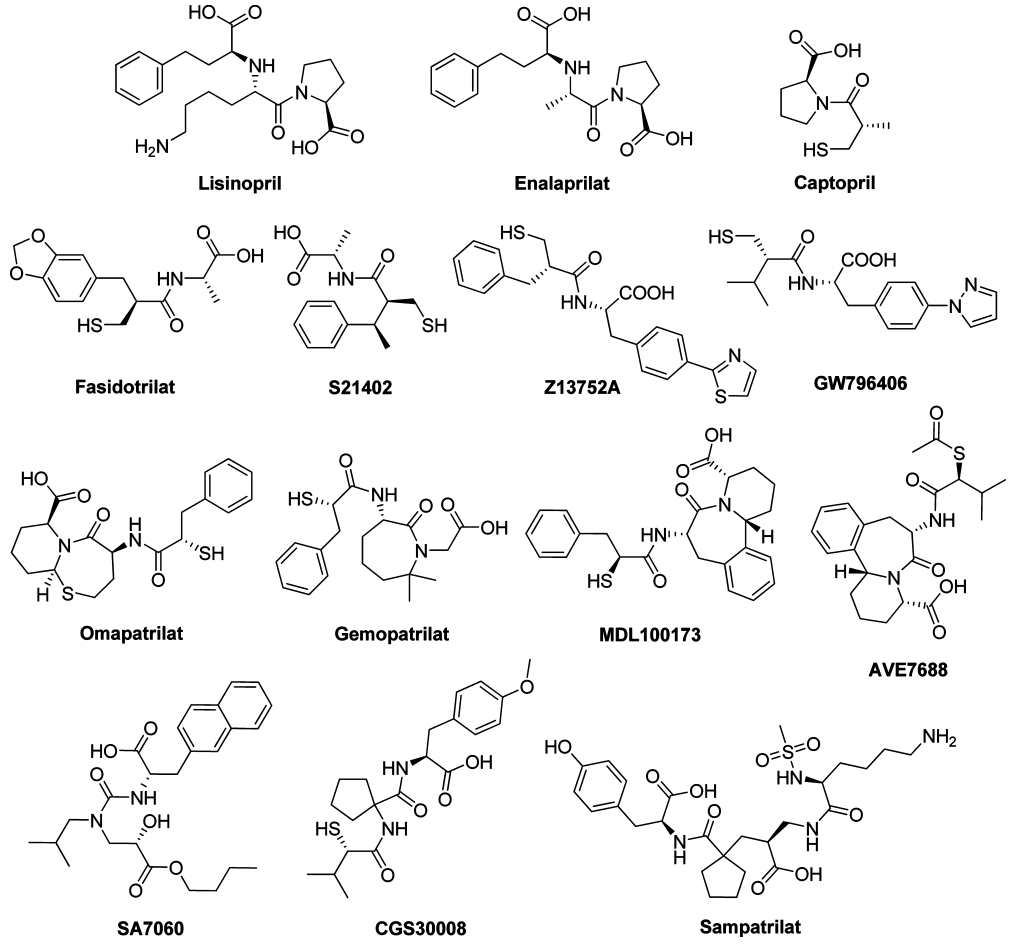

Table 1. Docking Results of the Three ACE Inhibitors with Available X-Ray Structures

ID	ligand	enzyme	rank[a]	rmsd[b] (Å)	ΔG_{calc}[c] (kcal mol^{-1})	ΔG_{exp}[c] (kcal mol^{-1})	K_{icalc} (nM)	K_{iexp} (nM)	ref
1	lisinopril	cACE	4	1.39	−13.98	−11.75	0.06	2.4	14, 42, 43
		nACE	1	1.40	−10.30	−10.03	28.3	44	
2	enalaprilat	cACE	3	0.95	−14.72	−11.18	0.02	6.3	14, 42, 43
		nACE	1	n/a[d]	−11.43	−10.34	4.2	26	
3	captopril	cACE	1	1.16	−11.35	−10.71	4.8	14	13, 43−45
		nACE	1	n/a[d]	−8.91	−10.98	296	8.9	

[a] Conformation rank by increasing docking energy. [b] Heavy atoms root-mean-square deviation with respect to the experimental structure. [c] The change in binding free energy is related to the inhibition constant using the equation: $\Delta G = RT \ln K_i$, where R is the gas constant 1.987 cal K^{-1} mol^{-1}, and T is the absolute temperature assumed to be 298.15 K. [d] X-ray structure not available.

Docked conformations were clustered within 1.0 Å root-mean-square positional deviation (rmsd). The program VMD 1.8.6[40] was used for analysis and preparation of the figures. All calculations were carried out on Intel Xeon processors, running x86 Linux 2.6.16 kernels. AutoDock 3.05 was compiled with gcc3.4 and Amber 9 using Intel Fortran 9.1.

RESULTS

Lisinopril, enalaprilat, and captopril (Scheme 1) are classified among the first generation clinical ACE inhibitors, and their crystal structures with ACE have been solved.[28,41] It should be noted that, for convenience, we refer to cACE using the numbering of testis ACE, since their sequences are virtually identical (amino acid numbering differs by 576)[8] and that the available crystal structures of "cACE-inhibitor" complexes have been obtained with testis ACE.[28,41]

In order to validate the docking method that is used in this study, we initially performed flexible docking of these three inhibitors with both domains of ACE. Our results were evaluated by means of: (i) the root-mean-square deviation (rmsd) of the best predicted solution with respect to the X-ray position of the inhibitors, and (ii) comparison of the predicted versus the experimental inhibition constants. The predictive ability for the binding mode of these three ligands is exemplified by the average rmsd = 1.23 Å, and the average difference of the free energy change of binding $\Delta(\Delta G)_{exp\text{-}calc} = 1.64$ kcal mol^{-1} (Table 1), which is within the residual standard error of AutoDock (2.18 kcal mol^{-1}).[38]

Lisinopril has been cocrystallized with both ACE domains (PDB ID: 1O86 for cACE[28] and 2C6N for nACE[29]). The selected docked conformations exhibit rmsds ∼ 1.4 Å with respect to their similar crystallographic positions in cACE and nACE (Figure 1A and B, respectively). Regarding the cACE−lisinopril complex, the fourth-ranked conformation (Table 1) was chosen as a result of its agreement with the crystal structure. Although the free energy of binding for

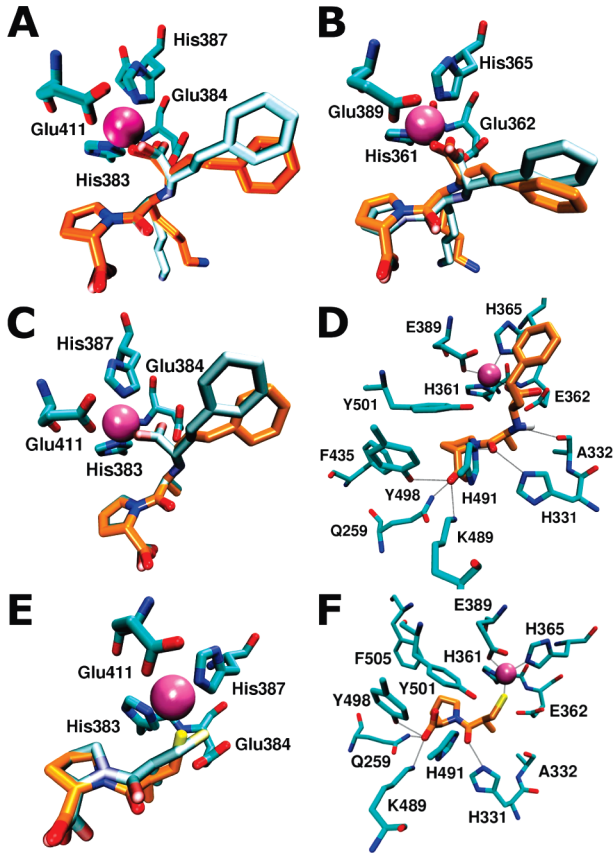

Figure 1. Comparison of the docked (orange carbon atoms) and crystallographic (light-cyan) conformations of: (A) cACE−lisinopril, (B) nACE−lisinopril, (C) cACE−enalaprilat, and (E) cACE−captopril complexes. Panels D and F show the predicted nACE−enalaprilat and nACE−captopril complexes, respectively. Key residues comprising the S_1-S_2' subsites are shown with carbon atoms in cyan. For all enzymes and inhibitors, the nitrogen atoms are blue, the oxygen atoms are red, and the sulfur atoms are yellow, and the catalytic zinc is shown as a mauve sphere.

the cACE-lisinopril complex deviates by 2.2 kcal mol^{-1} from the experimental value, the relative affinity of the inhibitor for the two domains is correctly estimated. Therefore, lisinopril is predicted to bind more strongly to cACE than to nACE, consistent with the experimental K_i of 2.4 nM for cACE and 44 nM for nACE (Table 1). Remarkably, the AutoDock scoring function was able to calculate the free energy of binding for the nACE−lisinopril complex within ~0.3 kcal mol^{-1} from ΔG_{exp}.

The correct modeling of the crystal structure of cACE−enalaprilat complex (PDB ID: 1UZE,[41] Figure 1C), with rmsd = 0.95 Å, was achieved in the third-ranked conformation (Table 1). Despite the fact that the K_i is overestimated for the cACE−enalaprilat complex (Table 1), the relative binding affinity of the inhibitor for the two domains is correctly predicted. The top-ranked conformation of nACE−enalaprilat complex (no X-ray structure available) is in good agreement with the experimental value (K_{iexp} = 26 nM versus K_{ical} = 4.2 nM). The central carboxylate group of enalaprilat is predicted to bind to the catalytic Zn^{2+} (Figure 1D). The terminal carboxylate forms a salt bridge with Lys489 (Lys511 in cACE) and two hydrogen bonds with Gln259 and Tyr498 (Gln281 and Tyr520 in cACE). Hydrogen bonds were also observed between the amide carbonyl group of enalaprilat and the protonated $N^{\varepsilon 2}$ of His331 (His353 in cACE) as well as between the secondary amine of enalaprilat and the C═O group of Ala332 (Ala354 in cACE). The proline moiety makes van der Waals contacts with Phe435 (Phe457), His491 (His513), Tyr498 (Tyr520), and Tyr501 (Tyr523), while the benzyl ring interacts with His365 (His387) and Thr496 (Val518).

The top-ranked conformation of captopril bound to cACE was within 1.16 Å rmsd of the crystallographic structure (PDB ID: 1UZF,[41] Figure 1E), and its predicted free energy of binding was overestimated by ~0.6 kcal mol^{-1} (Table 1). The top-ranked solution for the nACE−captopril complex, for which there is no crystallographic data, is predicted to have a K_{ical} = 296 nM compared to the experimental value of K_{iexp} = 8.9 nM. The binding mode of captopril is predicted to be similar in both cACE and nACE catalytic sites (Figure 1F). In particular, the thiolate of captopril makes a direct interaction with the catalytic Zn^{2+} ion at the active site of nACE and can also accept a hydrogen bond from Tyr501. Its terminal carboxylate group forms a salt bridge with Lys489 and two hydrogen bonds with the side chain amine of Gln259 and the hydroxyl group of Tyr498. The amide C═O is held by a hydrogen bond from His331. The proline moiety of captopril makes van der Waals contacts with Phe435, His491, Tyr501, and Phe505 (Phe527 in cACE), while the methyl group interacts with His361, Ala332, and Thr358 (Val380 in cACE).

Dual ACE/NEP Inhibitors. Docking simulations were performed for 11 dual ACE/NEP inhibitors with cACE, nACE, and NEP. The residue-specific interactions of each inhibitor are summarized in Table 2, whereas a detailed description of their binding modes is presented in the Supporting Information (Figures S1−S13). The energetic results for the selected conformations of each enzyme−ligand complex in comparison to the biological data[46−64] are summarized in the Supporting Information (Table S1). Here, we briefly describe the binding mode of three representative inhibitors: fasidotrilat, gemopatrilat, and MDL100173.

The top-ranked docked conformations of fasidotrilat complexed with cACE, nACE, and NEP (Figure 2A−C, respectively) revealed that the thiolate binds to the catalytic Zn^{2+}. The carboxylate group forms a salt bridge with Lys511 in cACE, with Lys489 in nACE, and with Arg110 in NEP. The carboxylate and the amide C═O group participate in several hydrogen bonds with Gln281, His353, His513, Tyr520 in cACE, with Gln259, His331, His491, Tyr498 in nACE, and with Asn542, Arg717 in NEP. The methylenedioxyphenyl moiety makes van der Waals contacts with hydrophobic residues in every one of the three enzymes.

Gemopatrilat is predicted to bind to Zn^{2+} of cACE, nACE, and NEP (Figure 3A−C, respectively) via its central carbonyl, located next to the SH group. This is quite different from fasidotrilat, which has the sulphydryl as the Zn^{2+}-coordinating group. On the other hand, the carboxylate group and the azepanone C═O exhibit similar electrostatic contacts with fasidotrilat. Additionally, the amide NH is hydrogen bonded to Ala354 in cACE, Ala332 in nACE, and Ala543 in NEP, while the SH group is bonded to Ala356, Glu384 in cACE, to Ala334, Glu362 in nACE, and to Tyr545, Glu584 in NEP. The azepanone moiety and the benzyl ring display several van der Waals interactions.

MDL100173 binds to the catalytic Zn^{2+} of cACE and nACE (Figure 4A and B, respectively) through the central amide C═O, located next to the SH group. Conversely, in

Table 2. Residue-Specific Interactions of the Dual ACE/NEP Inhibitors with the Catalytic Site of cACE, nACE, and NEP[a]

	cACE	nACE	NEP
fasidotrilat	**Gln281 His353** Val379 Val380 His383 Phe457 Lys511 **His513 Tyr520 Tyr523**	**Gln259 His331** Ser357 Thr358 His361 Phe435 Lys489 **His491 Tyr498 Tyr501**	Phe106 Arg110 **Asn542** Phe563 Met579 Val580 His583 Val692 **Trp693** Phe689 **His711 Arg717**
S21402	**Gln281 His353** Ala354 Val380 His383 Phe457 Lys511 **His513 Tyr520** Tyr523	**Gln259 His331** Ala332 Thr358 His361 Phe435 Lys489 **His491 Tyr498 Tyr501**	Phe106 Arg110 **Asn542** Ala543 Ile558 Phe563 Met579 Val580 His583 Val692 Trp693 Phe689 **His711 Arg717**
Z13752A	**Gln281** Thr282 **His353** Ala354 Val379 Val380 His383 **Lys454** Lys511 **His513 Tyr520**	**Gln259 His331** Ala332 Thr358 His361 Lys489 **His491 Tyr498 Tyr501**	**Asn542 Tyr545** Ile558 Phe563 Met579 Val580 His583 **Glu584** Val692 Trp693 Phe689 **His711** Arg717
GW796406	**Gln281** Thr282 His353 Ala354 Val380 His383 Lys511 **Tyr520 Tyr523**	**Gln259 His331** Thr358 Ala396 Lys489 Phe490 His491 Thr496 **Tyr498** Phe505	Phe106 **Asn542** Phe544 **Tyr545** Ile558 Phe563 Met579 Val580 His583 **Glu584** Val692 Trp693 Phe689 **His711** Arg717
omapatrilat	**Gln281 His353 Ala354 Ala356**> Val380 His383 **Glu384** Phe457 Lys511 Phe512 **His513** Val518 **Tyr520** Phe527	**Gln259 His331 Ala332 Ala334** Trp335 Thr358 His361 **Glu362** Phe435 Lys489 Phe490 **His491 Tyr498 Tyr501** Phe505	**Arg102** Phe106 Arg110 **Asn542** Ala543 Ile558 Phe563 Val580 His583 Trp693 **His711 Arg717**
gemopatrilat	**Gln281 His353 Ala354 Ala356** Trp357 Val380 His383 **Glu384** Phe457 Lys511 Phe512 **His513 Tyr520** Tyr523	**Gln259 His331 Ala332 Ala334** Trp335 Thr358 His361 **Glu362** Lys489 Phe490 **His491 Tyr498** Tyr501 Phe505	Phe106 Arg110 **Asn542 Ala543** Phe544 **Tyr545** Ile558 Val580 **Glu584** Trp693 His711
MDL100173	**Gln281 His353 Ala354 Ala356** Val380 His383 **Glu384** Phe457 Lys511 Phe512 **His513** Val518 **Tyr520** Tyr523	**Gln259 His331 Ala332 Ala334** Trp335 Thr358 His361 **Glu362** Phe435 Lys489 Phe490 **His491 Tyr498** Tyr501 Phe505	Phe106 **Ala543** Tyr545 Ile558 Phe563 Val580 His583 His587 Trp693 **His711** Arg717
AVE7688	**Gln281 His353 Ala354 Ala356** Val380 His383 **Glu384** Phe457 Lys511 Phe512 **His513** Val518 **Tyr520 Tyr523**	**Gln259 His331 Ala332 Ala334** Thr358 His361 **Glu362** Phe435 Lys489 Phe490 **His491** Thr496 **Tyr498** Tyr501 Phe505	Phe106 **Ala543** Phe544 Tyr545 Ile558 Phe563 Val580 His583 His587 Trp693 **His711** Arg717
SA7060	Val351 His353 **Ala356** Trp357 Phe391 Pro407 His410 Phe512 Val518 **Arg522 Tyr523** Phe570	Leu139 His331 **Ala332** Phe435 Phe490 **His491** Thr496 Tyr498 Tyr501	Val540 **Asn542** Phe544 Phe563 Met579 Val580 His583 His587 Val692 Trp693 Phe689 Arg717
CGS30008	**Gln281 His353 Ala354** Val380 His383 **Glu384** Phe457 Lys511 Phe512 **His513** Val518 **Tyr520 Tyr523** Phe527	**Gln259 His331 Ala332** Thr358 His361 **Glu362** Phe435 Lys489 Phe490 **His491** Thr496 Tyr501 Phe505	**Arg102** Phe106 **Asn542** Ile558 Phe563 Met579 Val580 His583 Val692 **Trp693 Asp709 His711**
sampatrilat	Glu162 **Gln281 His353** Ala354 Ala356 Asp377 Val380 His383 His387 Lys511 **His513** Val518 **Tyr520** Tyr523	Asp43 **Ser260** Val329 His331 Ala332 **Ala334** Trp335 Thr358 Phe490 His491 Thr496	**Asn542** Ala543 Phe544 **Tyr545** Ile558 Phe563 Val580 His583 Asp590 Asp591 Trp693 **His711** Arg717

[a] Residues involved in salt bridge interactions are underlined, those forming hydrogen bonds are in bold, and those involved in van der Waals interactions are in plain font.

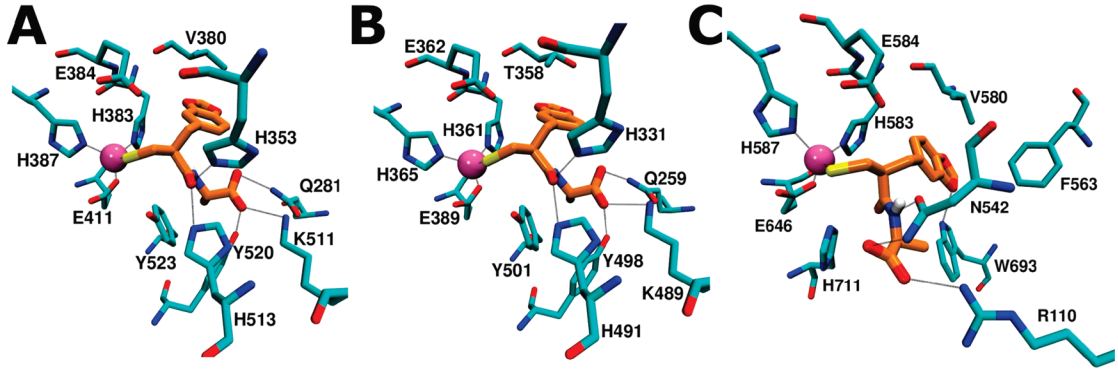

Figure 2. Simulated complex of fasidotrilat with: (A) cACE, (B) nACE, and (C) NEP. The inhibitor is shown with carbon atoms in orange sticks, while the surrounding residues are shown in cyan sticks. For all enzymes and inhibitors, the nitrogen atoms are blue, the oxygen atoms are red, and the sulfur atoms are yellow, and the catalytic zinc is shown as a mauve sphere.

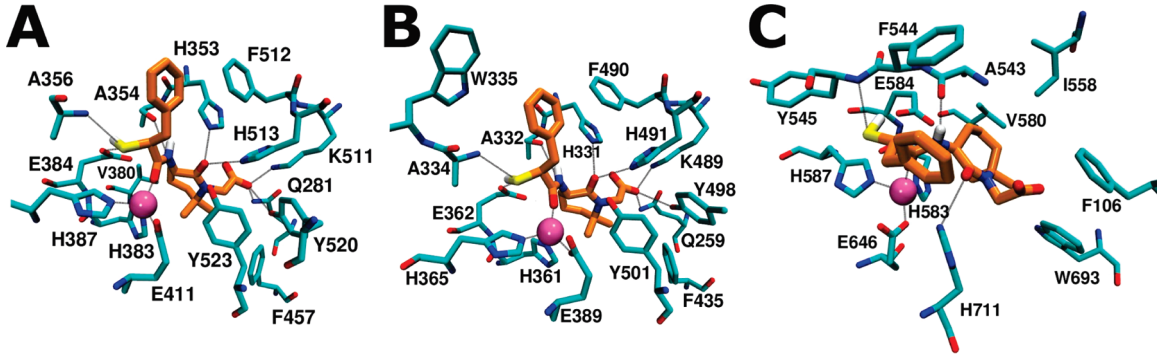

Figure 3. Simulated complex of gemopatrilat with: (A) cACE, (B) nACE, and (C) NEP. Atoms' colors are as in Figure 2.

the case of NEP, the catalytic Zn^{2+} is coordinated by both carbonyl groups of the inhibitor (Figure 4C). The carboxylate group forms a salt bridge with Lys511 in cACE, with Lys489 in nACE and with Arg717 in NEP, similar to fasidotrilat and gemopatrilat. In the case of cACE−nACE, the amide NH, the azepanone C═O, and the SH group form hydrogen bonds similar to gemopatrilat. The polycyclic moiety also interacts with Val380, Phe457, Tyr520, and Tyr523 in cACE

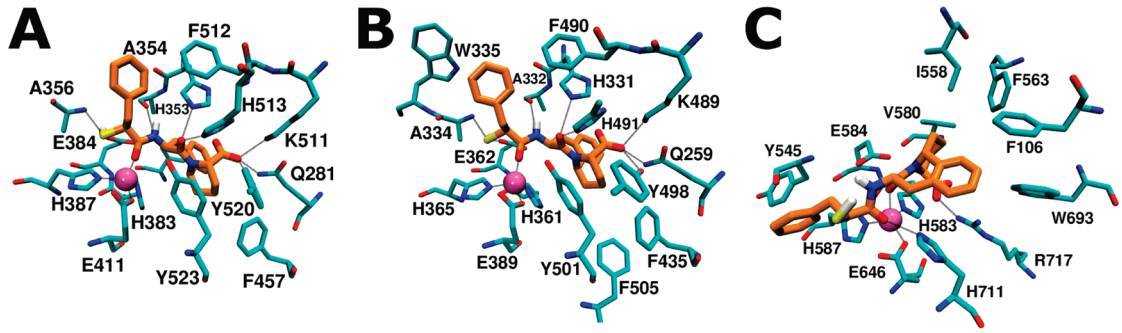

Figure 4. Simulated complex of MDL100173 with: (A) cACE, (B) nACE, and (C) NEP. Atoms' colors are as in Figure 2.

and with Phe435, Tyr498, Tyr501, and Phe505 in nACE. In the MDL100173-NEP complex, the amide C═O forms a hydrogen bond with His711, while the adjacent NH forms a hydrogen bond with Ala543. The van der Waals contacts are displayed between the polycyclic moiety and Phe106, Ile558, Phe563, Val580, and Trp693.

DISCUSSION

The limitations of empirical scoring functions (molecular mechanics force field-based) in accurately determining the free energy of binding of small molecule inhibitors have been well documented over the last years.[65−70] Their weakness can be overcome by more sophisticated and time-demanding methods, which have been developed and utilized to calculate a protein−ligand binding free energy with greater accuracy.[71−75] However, in our study, the empirical scoring function of AutoDock has proven to be adequate in determining the relative binding affinity of the three ACE inhibitors between the two highly homologous domains and within an average $\Delta(\Delta G)_{\text{exp-cal}} \sim 1.6$ kcal/mol (Table 1). What is more interesting for the scope of this work is the fact that correct binding modes were reproduced within the top four ranked docking solutions with a mean rmsd of 1.1 Å, with respect to the available crystallographic structures (Table 1).

A series of docking calculations of the dual ACE/NEP inhibitors posed in the catalytic groove of ACE and NEP provided insights into the inhibitory properties of ACE/NEP with potential inhibitors for simultaneous action on both enzymes. The docking solutions for the dual inhibitors indicate that fasidotrilat, S21402, and gemopatrilat have the same zinc-binding groups for both ACE and NEP, while for Z13752A, GW796406, omapatrilat, MDL100173, and AVE7688 inhibitors, the corresponding binding modes for ACE and NEP are different. The last three inhibitors (SA7060, CGS30008, and sampatrilat) do not fall into any of these categories due to their large number of flexible torsions and to many different putative zinc-binding groups.

Docking calculations for the dual ACE/NEP inhibitors indicate that there are two common zinc-binding groups and corresponding binding modes for ACE (both cACE and nACE). The catalytic zinc is coordinated by either the deprotonated SH group (fasidotrilat, S21402, Z13752A, and GW796406) or the central amide carbonyl group of the inhibitor (omapatrilat, gemopatrilat, MDL100173, and AVE7688). The inhibitors that belong to the same category share similar residue-specific interactions. In the first group (zinc coordinated by deprotonated SH, Figure 5A), the main interactions observed for cACE/nACE are: (i) the central

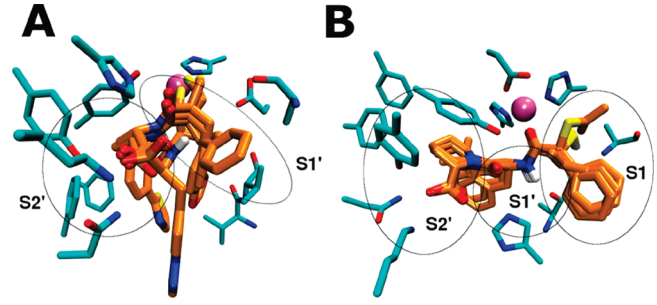

Figure 5. Overlay of the dual inhibitors models (orange sticks) bound to cACE (cyan sticks) active site residues. The catalytic Zn ion is represented as a mauve sphere. The catalytic zinc of cACE is coordinated by: (A) the deprotonated SH group of fasidotrilat, S21402, Z13752A, and GW796406 inhibitors, and (B) the central amide carbonyl group of the inhibitors omapatrilat, gemopatrilat, MDL100173, and AVE7688.

amide carbonyl is hydrogen bonded to His353/331 and His513/491 in subsite S_1', (ii) the carboxylate group binds to Lys511/489, Gln281/259, and Tyr520/498 in subsite S_2', and (iii) a bulky hydrophobic group is accommodated in subsite S_1'. In the second group (zinc coordinated by central C═O, Figure 5B), the main interactions are: (i) the central amide NH binds to Ala354/332 in subsite S_1', (ii) the C═O of the hydrophobic group is hydrogen bonded to His353/331 and His513/491 in subsite S_1', (iii) the terminal carboxylate binds to Lys511/489, Gln281/259, and Tyr520/498 in subsite S_2', (iv) a bulky hydrophobic group is accommodated in subsites $S_1'-S_2'$, (v) the SH group interacts with Ala356/334 and Glu384/362 in subsite S_1, and (vi) a benzyl group is accommodated in subsite S_1. An interesting thing to note is that the binding mode of the first group is similar to that of captopril, while the second group resembles that of lisinopril and enalaprilat.

The common interaction sites for both groups are the carboxylate group situated in S_2', the amide carbonyl in S_1', and the hydrophobic group in S_1'. The inhibitors of the second group possess an N-terminal benzyl moiety (with the exception of AVE7688, which has an isopropyl group in its place) that is accommodated by a hydrophobic pocket in S_1, comprised of His353/331, Trp357/335, Phe512/490, and Val518/Thr496 as well as exhibiting hydrogen bonds between their SH group and the residues Ala356/334 and Glu384/362. The additional interactions observed in S_1 subsite for the second group of inhibitors probably contribute to their lower predicted K_i values (for both ACE domains) compared to those of the first group, with the exception of Z13752A (Supporting Information, Table S1). The lower affinity of the first group of inhibitors is consistent with the structure−activity relationships for ACE inhibitors, which

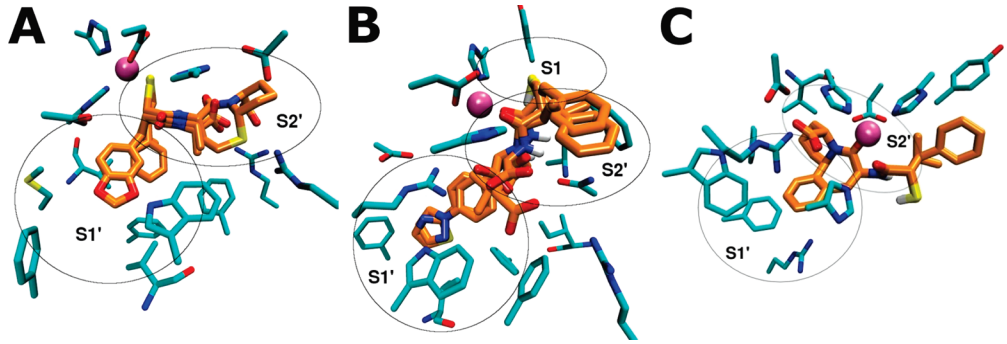

Figure 6. Overlay of the dual inhibitors models (orange sticks) bound to NEP (cyan sticks) active site residues. The catalytic Zn ion is represented as a mauve sphere. The catalytic zinc of NEP is coordinated by: (A) the deprotonated SH group of fasidotrilat, S21402, and omapatrilat, (B) by the amide carbonyl of Z13752A, GW796406, and gemopatrilat, and (C) the C═O of the azepanone ring of MDL100173 and AVE7688 dual inhibitors.

indicated that for optimal binding to the enzyme, the S_1 interaction is required.[13,14,45] Therefore, the potency of the inhibitors can be enhanced by a bulky hydrophobic group and a hydrogen-bonding group positioned in the S_1 subsite.

There are no experimental data regarding the affinities of the dual ACE/NEP inhibitors for each domain of ACE individually. In our study, the inhibitors were predicted to bind to the C-domain of ACE with greater affinity than the N-domain, with an average difference of the free energy of binding $\sim 2-3$ kcal mol^{-1} (Supporting Information, Table S1). The different affinities can be attributed to residue alterations between the two domains. In particular, the alteration of Val518 in the C-domain to Thr496 in the N-domain, located in the S_1 hydrophobic pocket, does not favor interactions with the P_1 benzyl group of the inhibitors. Moreover, the hydrophobic interactions of the residues Val380 (S_1') and Val379 (S_2') of cACE with the P_1' and P_2' groups are lost with the replacement by Thr358 and Ser357, respectively, in nACE. The same is true for the Thr282/Ser260 substitution in the S_2' subsite. These interactions confer C-domain selectivity to inhibitors which bear bulky hydrophobic groups in these positions.

The docking calculations for the NEP−inhibitor complexes indicate that there are three groups of inhibitor-binding modes. The first group (Figure 6A) consists of fasidotrilat, S21402, and omapatrilat, with the deprotonated sulfhydryl as the zinc-coordinating group. The key interactions are: (i) the terminal carboxylate binds to Arg110 and Asn542 in subsite S_2', (ii) the central amide C═O and NH groups are hydrogen bonded to Arg717 and Asn542, respectively, in subsite S_2', and (iii) a hydrophobic group is accommodated in S_1'. The second group (Figure 6B) includes Z13752A, GW796406 and gemopatrilat. The catalytic Zn^{2+} is coordinated by the amide carbonyl, while the main interactions are: (i) the carboxylate group binds to an arginine residue (Arg110 for gemopatrilat and Arg717 for Z13752A and GW796406) in subsite S_2', (ii) the amide NH is held by a hydrogen bond in subsite S_2', (iii) a bulky hydrophobic group is accommodated in S_1', (iv) the SH group is hydrogen bonded to Tyr545 and Glu584 in subsite S_1, and (v) a benzyl group is accommodated in S_2'. The third group (Figure 6C) includes MDL100173 and AVE7688, and they bind to the catalytic Zn^{2+} via both their carbonyl groups. The key interactions are: (i) the terminal carboxylate forms a salt bridge with Arg717 in subsite S_2', (ii) the central amide C═O and NH groups form hydrogen bonds in subsite S_2', and (iii) a bulky hydrophobic group is accommodated in S_1'.

The interactions shared by the above groups are a carboxylate group located in S_2', a central amide NH in S_2', and a hydrophobic group accommodated in subsite S_1'. These interactions are responsible for tight binding of the inhibitors, consistent with the structural features of the NEP−phosphoramidon crystallized complex.[16] On the other hand, the subsite S_1 interactions (hydrogen bonds with residues Tyr545 and Glu584) exhibited by some of the inhibitors (Z13752A, GW796406, and gemopatrilat) are of minor importance for substrate binding. These findings should be taken into account for future structure-based drug design.

CONCLUSION

This is the first comprehensive molecular docking study of eleven dual ACE/NEP inhibitors with cACE, nACE, and NEP. In the case of ACE, the docked structures can be divided into two groups based on their zinc coordination: (i) fasidotrilat, S21402, Z13752A, and GW796406 that bind the catalytic zinc via the deprotonated sulfhydryl and (ii) omapatrilat, gemopatrilat, MDL100173, and AVE7688 which are coordinated by the central amide carbonyl group of the inhibitor. The NEP−inhibitor complexes showed that there are three possible zinc coordinator groups: (i) fasidotrilat, S21402, and omapatrilat that bind the catalytic zinc via a deprotonated sulfhydryl, (ii) gemopatrilat, Z13752A, and GW796406 that are coordinated by their amide carbonyl, and (iii) MDL100173 and AVE7688 where the zinc is coordinated by both carbonyl groups of the molecule. Furthermore, we have made an attempt to provide a structural basis for the observed differences in the binding affinity of dual ACE/NEP inhibitors. These findings are particularly relevant considering the shadow cast over the ACE/NEP inhibitors by omapatrilat and the increased incidence of angioedema. Insights from the molecular docking with the N- and C-domain active sites open the door for the design of novel cACE/NEP inhibitors that would still allow the N-domain to hydrolyze BK and, thus, improve the side-effect profile of the drug. Moreover, nACE/NEP dual inhibitors could have antihypertensive and antifibrotic activities, the latter largely due to elevated AcSDKP levels. These structure-based approaches to drug development embrace the emerging field of personalized medicine and may lead to improved dual inhibitors and to next generation drugs.

Supporting Information Available: Table S1: Docking results of the dual ACE/NEP inhibitors (docking rank, free

energy change of binding, inhibition constant). Pages S3−S15: Detailed analysis of all enzyme−inhibitor interactions with Figures S1−S13. This information is available free of charge via the Internet at http://pubs.acs.org/.

REFERENCES AND NOTES

(1) Kearney, P. M.; Whelton, M.; Reynolds, K.; Muntner, P.; Whelton, P. K.; He, J. Global burden of hypertension: analysis of worldwide data. *Lancet* **2005**, *365*, 217–223.

(2) Jones, D. W.; Hall, J. E. Seventh report of the Joint National Committee on Prevention, Detection, Evaluation, and Treatment of High Blood Pressure and evidence from new hypertension trials. *Hypertension* **2004**, *43*, 1–3.

(3) Cargill, R. I.; Lipworth, B. J. The role of the renin-angiotensin and natriuretic peptide systems in the pulmonary vasculature. *Br. J. Clin. Pharmacol.* **1995**, *40*, 11–18.

(4) Daull, P.; Jeng, A. Y.; Battistini, B. Towards triple vasopeptidase inhibitors for the treatment of cardiovascular diseases. *J. Cardiovasc. Pharmacol.* **2007**, *50*, 247–256.

(5) Sturrock, E. D.; Natesh, R.; van Rooyen, J. M.; Acharya, K. R. Structure of angiotensin I-converting enzyme. *Cell. Mol. Life Sci.* **2004**, *61*, 2677–2686.

(6) Acharya, K. R.; Sturrock, E. D.; Riordan, J. F.; Ehlers, M. R. Ace revisited: a new target for structure-based drug design. *Nat. Rev. Drug Discov.* **2003**, *2*, 891–902.

(7) Hubert, C.; Houot, A. M.; Corvol, P.; Soubrier, F. Structure of the angiotensin I-converting enzyme gene. Two alternate promoters correspond to evolutionary steps of a duplicated gene. *J. Biol. Chem.* **1991**, *266*, 15377–15383.

(8) Ehlers, M. R.; Fox, E. A.; Strydom, D. J.; Riordan, J. F. Molecular cloning of human testicular angiotensin-converting enzyme: the testis isozyme is identical to the C-terminal half of endothelial angiotensin-converting enzyme. *Proc. Natl. Acad. Sci. U.S.A.* **1989**, *86*, 7741–7745.

(9) Soubrier, F.; Alhenc-Gelas, F.; Hubert, C.; Allegrini, J.; John, M.; Tregear, G.; Corvol, P. Two putative active centers in human angiotensin I-converting enzyme revealed by molecular cloning. *Proc. Natl. Acad. Sci. U.S.A.* **1988**, *85*, 9386–9390.

(10) Wei, L.; Alhenc-Gelas, F.; Corvol, P.; Clauser, E. The two homologous domains of human angiotensin I-converting enzyme are both catalytically active. *J. Biol. Chem.* **1991**, *266*, 9002–9008.

(11) Jaspard, E.; Wei, L.; Alhenc-Gelas, F. Differences in the properties and enzymatic specificities of the two active sites of angiotensin I-converting enzyme (kininase II). Studies with bradykinin and other natural peptides. *J. Biol. Chem.* **1993**, *268*, 9496–9503.

(12) Georgiadis, D.; Beau, F.; Czarny, B.; Cotton, J.; Yiotakis, A.; Dive, V. Roles of the two active sites of somatic angiotensin-converting enzyme in the cleavage of angiotensin I and bradykinin: insights from selective inhibitors. *Circ. Res.* **2003**, *93*, 148–154.

(13) Ondetti, M. A.; Rubin, B.; Cushman, D. W. Design of specific inhibitors of angiotensin-converting enzyme: new class of orally active antihypertensive agents. *Science* **1977**, *196*, 441–444.

(14) Patchett, A. A.; Harris, E.; Tristram, E. W.; Wyvratt, M. J.; Wu, M. T.; Taub, D.; Peterson, E. R.; Ikeler, T. J.; ten Broeke, J.; Payne, L. G.; Ondeyka, D. L.; Thorsett, E. D.; Greenlee, W. J.; Lohr, N. S.; Hoffsommer, R. D.; Joshua, H.; Ruyle, W. V.; Rothrock, J. W.; Aster, S. D.; Maycock, A. L.; Robinson, F. M.; Hirschmann, R.; Sweet, C. S.; Ulm, E. H.; Gross, D. M.; Vassil, T. C.; Stone, C. A. A new class of angiotensin-converting enzyme inhibitors. *Nature* **1980**, *288*, 280–283.

(15) Roques, B. P.; Noble, F.; Dauge, V.; Fournie-Zaluski, M. C.; Beaumont, A. Neutral endopeptidase 24.11: structure, inhibition, and experimental and clinical pharmacology. *Pharmacol. Rev.* **1993**, *45*, 87–146.

(16) Oefner, C.; D'Arcy, A.; Hennig, M.; Winkler, F. K.; Dale, G. E. Structure of human neutral endopeptidase (Neprilysin) complexed with phosphoramidon. *J. Mol. Biol.* **2000**, *296*, 341–349.

(17) Graf, K.; Koehne, P.; Grafe, M.; Zhang, M.; Auch-Schwelk, W.; Fleck, E. Regulation and differential expression of neutral endopeptidase 24.11 in human endothelial cells. *Hypertension* **1995**, *26*, 230–235.

(18) Iwata, N.; Tsubuki, S.; Takaki, Y.; Shirotani, K.; Lu, B.; Gerard, N. P.; Gerard, C.; Hama, E.; Lee, H. J.; Saido, T. C. Metabolic regulation of brain Abeta by neprilysin. *Science* **2001**, *292*, 1550–1552.

(19) Francis, F.; Hennig, S.; Korn, B.; Reinhardt, R.; de Jong, P.; Poustka, A.; Lehrach, H.; Powe, P. S. N.; Goulding, J. N.; Summerfield, T.; Mountford, R.; Read, A. P.; Popowska, E.; Pronicka, E.; Davies, K. E.; O'Riordan, J. L. H.; Econs, M. J.; Nesbitt, T.; Drezner, M. K.; Oudet, C.; Pannetier, S.; Hanauer, A.; Strom, T. M.; Meindl, A.; Lorenz, B.; Cagnoli, B.; Mohnike, K. L.; Murken, J.; Meitinger, T. A gene (PEX) with homologies to endopeptidases is mutated in patients with X-linked hypophosphatemic rickets. The HYP Consortium *Nat. Genet.* **1995**, *11*, 130−136.

(20) Roques, B. P.; Beaumont, A. Neutral endopeptidase-24.11 inhibitors: from analgesics to antihypertensives. *Trends Pharmacol. Sci.* **1990**, *11*, 245–249.

(21) Burnett, J. C., Jr. Vasopeptidase inhibition: a new concept in blood pressure management. *J. Hypertens. Suppl* **1999**, *17*, S37–43.

(22) Sagnella, G. A.; Markandu, N. D.; Buckley, M. G.; Miller, M. A.; Blackwood, A.; Singer, D. R.; MacGregor, G. A. Hormonal and renal responses to neutral endopeptidase inhibition in normal humans on a low and on a high sodium intake. *Eur. J. Clin. Invest* **1995**, *25*, 165–170.

(23) Northridge, D. B.; Newby, D. E.; Rooney, E.; Norrie, J.; Dargie, H. J. Comparison of the short-term effects of candoxatril, an orally active neutral endopeptidase inhibitor, and frusemide in the treatment of patients with chronic heart failure. *Am. Heart J.* **1999**, *138*, 1149–1157.

(24) Favrat, B.; Burnier, M.; Nussberger, J.; Lecomte, J. M.; Brouard, R.; Waeber, B.; Brunner, H. R. Neutral endopeptidase versus angiotensin converting enzyme inhibition in essential hypertension. *J. Hypertens.* **1995**, *13*, 797–804.

(25) Richards, A. M.; Wittert, G. A.; Crozier, I. G.; Espiner, E. A.; Yandle, T. G.; Ikram, H.; Frampton, C. Chronic inhibition of endopeptidase 24.11 in essential hypertension: evidence for enhanced atrial natriuretic peptide and angiotensin II. *J. Hypertens.* **1993**, *11*, 407–416.

(26) Bralet, J.; Schwartz, J. C. Vasopeptidase inhibitors: an emerging class of cardiovascular drugs. *Trends Pharmacol. Sci.* **2001**, *22*, 106–109.

(27) Zanchi, A.; Maillard, M.; Burnier, M. Recent clinical trials with omapatrilat: new developments. *Curr. Hypertens. Rep.* **2003**, *5*, 346–352.

(28) Natesh, R.; Schwager, S. L.; Sturrock, E. D.; Acharya, K. R. Crystal structure of the human angiotensin-converting enzyme-lisinopril complex. *Nature* **2003**, *421*, 551–554.

(29) Corradi, H. R.; Schwager, S. L.; Nchinda, A. T.; Sturrock, E. D.; Acharya, K. R. Crystal structure of the N domain of human somatic angiotensin I-converting enzyme provides a structural basis for domain-specific inhibitor design. *J. Mol. Biol.* **2006**, *357*, 964–974.

(30) Case, D. A.; Cheatham, T. E., III.; Darden, T.; Gohlke, H.; Luo, R.; Merz, K. M., Jr.; Onufriev, A.; Simmerling, C.; Wang, B.; Woods, R. J. The Amber biomolecular simulation programs. *J. Comput. Chem.* **2005**, *26*, 1668–1688.

(31) Bashford, D.; Karplus, M. pKa's of ionizable groups in proteins: atomic detail from a continuum electrostatic model. *Biochemistry* **1990**, *29*, 10219–10225.

(32) Hornak, V.; Abel, R.; Okur, A.; Strockbine, B.; Roitberg, A.; Simmerling, C. Comparison of multiple Amber force fields and development of improved protein backbone parameters. *Proteins* **2006**, *65*, 712–725.

(33) Papakyriakou, A.; Spyroulias, G. A.; Sturrock, E. D.; Manessi-Zoupa, E.; Cordopatis, P. Simulated interactions between angiotensin-converting enzyme and substrate gonadotropin-releasing hormone: novel insights into domain selectivity. *Biochemistry* **2007**, *46*, 8753–8765.

(34) Tsui, V.; Case, D. A. Theory and applications of the generalized Born solvation model in macromolecular Simulations. *Biopolymers* **2000**, *56*, 275–291.

(35) Jakalian, A.; Jack, D. B.; Bayly, C. I. Fast, efficient generation of high-quality atomic charges. AM1-BCC model: II Parameterization and validation. *J. Comput. Chem.* **2002**, *23*, 1623–1641.

(36) *Molcharge, version 1.3.1*; OpenEye Scientific Software Inc: Santa Fe, NM, 2005.

(37) Kirchmair, J.; Wolber, G.; Laggner, C.; Langer, T. Comparative performance assessment of the conformational model generators omega and catalyst: a large-scale survey on the retrieval of protein-bound ligand conformations. *J. Chem. Inf. Model.* **2006**, *46*, 1848–1861.

(38) Morris, G. M.; Goodsell, D. S.; Halliday, R. S.; Huey, R.; Hart, W. E.; Belew, R. K.; Olson, A. J. Automated docking using a Lamarckian genetic algorithm and an empirical binding free energy function. *J. Comput. Chem.* **1998**, *19*, 1639–1662.

(39) Sanner, M. F. Python: a programming language for software integration and development. *J. Mol. Graph. Model.* **1999**, *17*, 57–61.

(40) Humphrey, W.; Dalke, A.; Schulten, K. VMD: visual molecular dynamics. *J. Mol. Graph.* **1996**, *14* (33−38), 27–38.

(41) Natesh, R.; Schwager, S. L.; Evans, H. R.; Sturrock, E. D.; Acharya, K. R. Structural details on the binding of antihypertensive drugs captopril and enalaprilat to human testicular angiotensin I-converting enzyme. *Biochemistry* **2004**, *43*, 8718–8724.

(42) Patchett, A. A.; Cordes, E. H. The design and properties of N-carboxyalkyldipeptide inhibitors of angiotensin-converting enzyme. *Adv. Enzymol. Relat. Areas Mol. Biol.* **1985**, *57*, 1–84.

(43) Wei, L.; Clauser, E.; Alhenc-Gelas, F.; Corvol, P. The two homologous domains of human angiotensin I-converting enzyme interact differently with competitive inhibitors. *J. Biol. Chem.* **1992**, *267*, 13398–13405.

(44) Cushman, D. W.; Cheung, H. S.; Sabo, E. F.; Ondetti, M. A. Design of potent competitive inhibitors of angiotensin-converting enzyme. Carboxyalkanoyl and mercaptoalkanoyl amino acids. *Biochemistry* **1977**, *16*, 5484–5491.
(45) Cushman, D. W.; Ondetti, M. A. Design of angiotensin converting enzyme inhibitors. *Nature Medicine* **1999**, *5*, 1110–1112.
(46) Ozdener, F.; Ozdemir, V. Fasidotril Eli Lilly. *Curr. Opin. Investig. Drugs* **2003**, *4*, 1113–1119.
(47) Laurent, S.; Boutouyrie, P.; Azizi, M.; Marie, C.; Gros, C.; Schwartz, J. C.; Lecomte, J. M.; Bralet, J. Antihypertensive effects of fasidotril, a dual inhibitor of neprilysin and angiotensin-converting enzyme, in rats and humans. *Hypertension* **2000**, *35*, 1148–1153.
(48) Fournie-Zaluski, M. C.; Gonzalez, W.; Turcaud, S.; Pham, I.; Roques, B. P.; Michel, J. B. Dual inhibition of angiotensin-converting enzyme and neutral endopeptidase by the orally active inhibitor mixanpril: a potential therapeutic approach in hypertension. *Proc. Natl. Acad. Sci. U.S.A.* **1994**, *91*, 4072–4076.
(49) Bani, M.; Colantoni, A.; Guillaume, M.; Macchi, F.; Moroni, G.; Persiani, S. A double-blind, placebo-controlled study to assess tolerability, pharmacokinetics and preliminary pharmacodynamics of single escalating doses of Z13752A, a novel dual inhibitor of the metalloproteases ACE and NEP, in healthy volunteers. *Br. J. Clin. Pharmacol.* **2000**, *50*, 338–349.
(50) Sulpizio, A. C.; Pullen, M. A.; Edwards, R. M.; Louttit, J. B.; West, R.; Brooks, D. P. Mechanism of vasopeptidase inhibitor-induced plasma extravasation: comparison of omapatrilat and the novel neutral endopeptidase 24.11/angiotensin-converting enzyme inhibitor GW796406. *J. Pharmacol. Exp. Ther.* **2005**, *315*, 1306–1313.
(51) Tabrizchi, R. Omapatrilat. Bristol-Myers Squibb. *Curr. Opin. Investig. Drugs* **2001**, *2*, 1414–1422.
(52) Trippodo, N. C.; Robl, J. A.; Asaad, M. M.; Fox, M.; Panchal, B. C.; Schaeffer, T. R. Effects of omapatrilat in low, normal, and high renin experimental hypertension. *Am. J. Hypertens.* **1998**, *11*, 363–372.
(53) Packer, M.; Califf, R. M.; Konstam, M. A.; Krum, H.; McMurray, J. J.; Rouleau, J. L.; Swedberg, K. Comparison of omapatrilat and enalapril in patients with chronic heart failure: the Omapatrilat Versus Enalapril Randomized Trial of Utility in Reducing Events (OVERTURE). *Circulation* **2002**, *106*, 920–926.
(54) Robl, J. A.; Sulsky, R.; Sieber-McMaster, E.; Ryono, D. E.; Cimarusti, M. P.; Simpkins, L. M.; Karanewsky, D. S.; Chao, S.; Asaad, M. M.; Seymour, A. A.; Fox, M.; Smith, P. L.; Trippodo, N. C. Vasopeptidase inhibitors: incorporation of geminal and spirocyclic substituted azepinones in mercaptoacyl dipeptides. *J. Med. Chem.* **1999**, *42*, 305–311.
(55) Hubner, R. A.; Kubota, E.; Casley, D. J.; Johnston, C. I.; Burrell, L. M. In-vitro and in-vivo inhibition of rat neutral endopeptidase and angiotensin converting enzyme with the vasopeptidase inhibitor gemopatrilat. *J. Hypertens.* **2001**, *19*, 941–946.
(56) Laverman, G. D.; Van Goor, H.; Henning, R. H.; De Jong, P. E.; De Zeeuw, D.; Navis, G. Renoprotective effects of VPI versus ACEI in normotensive nephrotic rats on different sodium intakes. *Kidney Int.* **2003**, *63*, 64–71.
(57) French, J.; Flynn, G.; Giroux, E.; Mehdi, S.; Anderson, B.; Beach, D.; Koehl, J.; Dage, R. Characterization of a dual inhibitor of angiotensin I-converting enzyme and neutral endopeptidase. *J. Pharmacol. Exp. Ther.* **1994**, *268*, 180–186.
(58) Emmons, G. T.; Argenti, R.; Martin, L. L.; Martin, N. E.; Jensen, B. K. Pharmacokinetics of M100240 and MDL 100,173, a dual angiotensin-converting enzyme/neutral endopeptidase inhibitor, in healthy young and elderly volunteers. *J. Clin. Pharmacol.* **2004**, *44*, 901–905.
(59) Tabrizchi, R. Ilepatril (AVE-7688), a vasopeptidase inhibitor for the treatment of hypertension. *Curr. Opin. Investig. Drugs* **2008**, *9*, 301–309.
(60) Schafer, S.; Linz, W.; Vollert, H.; Biemer-Daub, G.; Rutten, H.; Bleich, M.; Busch, A. E. The vasopeptidase inhibitor AVE7688 ameliorates Type 2 diabetic nephropathy. *Diabetologia* **2004**, *47*, 98–103.
(61) Kuro, T.; Okahara, A.; Nose, M.; Ikuse, T.; Matsumura, Y. Effects of SA7060, a novel dual inhibitor of neutral endopeptidase and angiotensin-converting enzyme, on deoxycorticosterone acetate-salt-induced hypertension in rats. *Biol. Pharm. Bull.* **2000**, *23*, 820–825.
(62) Chatelain, R. E.; Ghai, R. D.; Trapani, A. J.; Odorico, L. M.; Dardik, B. N.; De Lombaert, S.; Lappe, R. W.; Fink, C. A. Antihypertensive and natriuretic effects of CGS 30440, a dual inhibitor of angiotensin-converting enzyme and neutral endopeptidase 24.11. *J. Pharmacol. Exp. Ther.* **1998**, *284*, 974–982.
(63) Allikmets, K. Sampatrilat Shire. *Curr. Opin. Investig. Drugs* **2002**, *3*, 578–581.
(64) Maki, T.; Nasa, Y.; Tanonaka, K.; Takahashi, M.; Takeo, S. Beneficial effects of sampatrilat, a novel vasopeptidase inhibitor, on cardiac remodeling and function of rats with chronic heart failure following left coronary artery ligation. *J. Pharmacol. Exp. Ther.* **2003**, *305*, 97–105.
(65) Bursulaya, B. D.; Totrov, M.; Abagyan, R.; Brooks, C. L. 3rd; Comparative study of several algorithms for flexible ligand docking. *J. Comput.-Aided Mol. Des.* **2003**, *17*, 755–763.
(66) Cross, J. B.; Thompson, D. C.; Rai, B. K.; Baber, J. C.; Fan, K. Y.; Hu, Y.; Humblet, C. Comparison of several molecular docking programs: pose prediction and virtual screening accuracy. *J. Chem. Inf. Model.* **2009**, *49*, 1455–1474.
(67) Cummings, M. D.; DesJarlais, R. L.; Gibbs, A. C.; Mohan, V.; Jaeger, E. P. Comparison of automated docking programs as virtual screening tools. *J. Med. Chem.* **2005**, *48*, 962–976.
(68) Kitchen, D. B.; Decornez, H.; Furr, J. R.; Bajorath, J. Docking and scoring in virtual screening for drug discovery: methods and applications. *Nat. Rev. Drug Discov.* **2004**, *3*, 935–949.
(69) Kontoyianni, M.; McClellan, L. M.; Sokol, G. S. Evaluation of docking performance: comparative data on docking algorithms. *J. Med. Chem.* **2004**, *47*, 558–565.
(70) Perola, E.; Walters, W. P.; Charifson, P. S. A detailed comparison of current docking and scoring methods on systems of pharmaceutical relevance. *Proteins* **2004**, *56*, 235–249.
(71) Gilson, M. K.; Zhou, H. X. Calculation of protein-ligand binding affinities. *Annu. Rev. Biophys. Biomol. Struct.* **2007**, *36*, 21–42.
(72) Pearlman, D. A. Evaluating the molecular mechanics poisson-boltzmann surface area free energy method using a congeneric series of ligands to p38 MAP kinase. *J. Med. Chem.* **2005**, *48*, 7796–7807.
(73) Oostenbrink, C.; van Gunsteren, W. F. Free energies of ligand binding for structurally diverse compounds. *Proc. Natl. Acad. Sci. U.S.A.* **2005**, *102*, 6750–6754.
(74) Woo, H. J.; Roux, B. Calculation of absolute protein-ligand binding free energy from computer simulations. *Proc. Natl. Acad. Sci. U.S.A.* **2005**, *102*, 6825–6830.
(75) Bash, P. A.; Singh, U. C.; Brown, F. K.; Langridge, R.; Kollman, P. A. Calculation of the relative change in binding free energy of a protein-inhibitor complex. *Science* **1987**, *235*, 574–576.

CI9005047